# 3. PHYSICAL CHARACTERISTICS

## 3.1 Morphometry

### Volume

Volume is a state variable and can be computed in several ways depending on availability of data and the site dynamics. It is important for computing the dilution or concentration of pollutants, nutrients, and organisms; it may be constant, but usually it is time varying. In the model, ponds, lakes, and reservoirs are treated differently than streams, especially with respect to computing volumes. The change in volume of ponds, lakes, and reservoirs is computed as:

$$\frac{dVolume}{dt} = Inflow - Discharge - Evap \tag{1}$$

where:

| | | |
|---|---|---|
| *dVolume/dt* | = | derivative for volume of water ($m^3$/d), |
| *Inflow* | = | inflow of water into waterbody ($m^3$/d), |
| *Discharge* | = | discharge of water from waterbody ($m^3$/d), and |
| *Evap* | = | evaporation ($m^3$/d), see **(2)**. |

Evaporation is converted from an annual value for the site to a daily value using the simple relationship:

$$Evap = \frac{MeanEvap}{365} \cdot 0.0254 \cdot Area \tag{2}$$

where:

| | | |
|---|---|---|
| *MeanEvap* | = | mean annual evaporation (in/yr), |
| 365 | = | days per year (yr), |
| 0.0254 | = | conversion from inches to meters (m/in), and |
| *Area* | = | area of the waterbody ($m^2$). |

The user is given several options for computing volume including keeping the volume constant; making the volume a dynamic function of inflow, discharge, and evaporation; using a time series of known values; and computing volume as a function of the Manning's equation. Depending on the method, inflow and discharge are varied, as indicated in **Table 1**.

**Table 1. Computation of Volume, Inflow, and Discharge**

| Method | Inflow | Discharge |
|---|---|---|
| Constant | *InflowLoad* | *InflowLoad - Evap* |
| Dynamic | *InflowLoad* | *DischargeLoad* |
| Known values | *InflowLoad* | *InflowLoad - Evap + (State - KnownVals)/dt* |
| Manning | *ManningVol - (State + Discharge)/dt + Evap* | *DischargeLoad* |

The variables are defined as:

| | | |
|---|---|---|
| *InflowLoad* | = | user-supplied inflow loading ($m^3/d$); |
| *DischargeLoad* | = | user-supplied discharge loading ($m^3/d$); |
| *State* | = | computed state variable value for volume ($m^3$); |
| *KnownVals* | = | time series of known values of volume ($m^3$); |
| *dt* | = | incremental time in simulation (d); and |
| *ManningVol* | = | volume of stream reach ($m^3$), see **(3)**. |

**Figure 12** illustrates time-varying volumes and inflow loadings specified by the user and discharge computed by the model for a run-of-the-river reservoir. Note that significant drops in volume occur with operational releases, usually in the spring, for flood control purposes.

**Figure 12**. Volume, Inflow, and Discharge for a 4-year Period in Coralville Reservoir, Iowa.

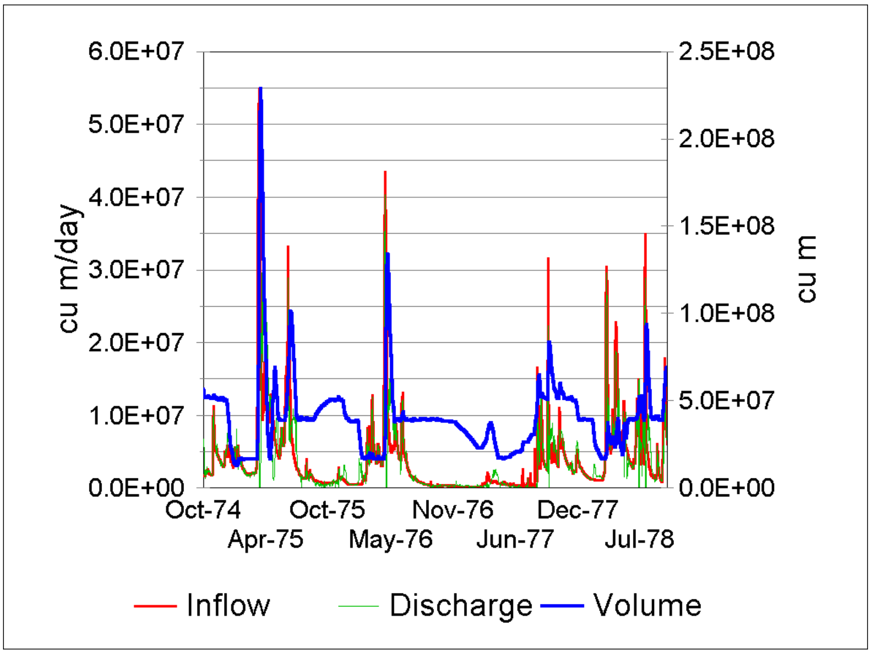


The time-varying volume of water in a stream channel is computed as:

$$ManningVol = Y \cdot CLength \cdot Width \tag{3}$$

where:

| | | |
|---|---|---|
| *Y* | = | dynamic mean depth (m), see **(4)**; |
| *CLength* | = | length of reach (m); and |
| *Width* | = | width of channel (m). |

In streams the depth of water and flow rate are key variables in computing the transport, scour, and deposition of sediments. Time-varying water depth is a function of the flow rate, channel roughness, slope, and channel width using Manning's equation:

$$Y = \left( \frac{Q \cdot Manning}{\sqrt{Slope} \cdot Width} \right)^{3/5} \tag{4}$$

where:

| | | |
|---|---|---|
| $Q$ | = | flow rate ($m^3/s$); |
| $Manning$ | = | Manning's roughness coefficient ($s/m^{1/3}$); |
| $Slope$ | = | slope of channel (m/m); and |
| $Width$ | = | channel width (m). |

The Manning's roughness coefficient is an important parameter representing frictional loss, but it is not subject to direct measurement. The user can choose among the following stream types:

- concrete channel (with a default Manning's coefficient of 0.020);
- dredged channel, such as ditches and channelized streams (default coefficient of 0.030); and
- natural channel (default coefficient of 0.040).

These generalities are based on Chow's (1959) tabulated values as given by Hoggan (1989).

In the absence of inflow data, the flow rate is computed from the initial mean water depth, assuming a rectangular channel and using a rearrangement of Manning's equation:

$$QBase = \frac{IDepth^{5/3} \cdot \sqrt{Slope} \cdot Width}{Manning} \tag{5}$$

where:

| | | |
|---|---|---|
| $QBase$ | = | base flow ($m^3/s$); and |
| $Idepth$ | = | mean depth as given in site record (m). |

The dynamic flow rate is calculated from the inflow loading by converting from $m^3/d$ to $m^3/s$:

$$Q = \frac{Inflow}{86400} \tag{6}$$

where:

| | | |
|---|---|---|
| $Q$ | = | flow rate ($m^3/s$); and |
| $Inflow$ | = | water discharged into channel from upstream ($m^3/d$). |

**Bathymetric Approximations**

The depth distribution of a water body is important because it determines the areas and volumes subject to mixing and light penetration. The shapes of ponds, lakes, reservoirs, and streams are represented in the model by idealized geometrical approximations, following the topological treatment of Junge (1966; see also Straškraba and Gnauck, 1985). The shape parameter *P* (Junge, 1966) characterizes the site, with a shape that is indicated by the ratio of mean to maximum depth.:

$$P = 6.0 \cdot \frac{ZMean}{ZMax} - 3.0 \tag{7}$$

Where:

| | | |
|---|---|---|
| *ZMean* | = | mean depth (m); |
| *ZMax* | = | maximum depth (m); and |
| *P* | = | characterizing parameter for shape (unitless).; *P* is constrained between -1.0 and 1.0 |

Shallow constructed ponds and ditches may be approximated by an ellipsoid where *Z/ZMax* = 0.6 and *P* = 0.6. Reservoirs generally are extreme elliptic sinusoids with values of *P* constrained to -1.0. Lakes may be either elliptic sinusoids, with *P* between 0.0 and -1.0, or elliptic hyperboloids with *P* between 0.0 and 1.0 (**Table 2**). The model requires mean and maximum depth, but if only the maximum depth is known, then the mean depth can be estimated by multiplying *ZMax* by the representative ratio. Not all water bodies fit the elliptic shapes, but the model generally is not sensitive to the deviations.

Based on these relationships, fractions of volumes and areas can be determined for any given depth (Junge, 1966) (**Figure 13**-**Figure 14**):

$$AreaFrac = (1.0 + P) \cdot \frac{Z}{ZMax} - P \cdot \left(\frac{Z}{ZMax}\right)^2 \tag{8}$$

$$VolFrac = \frac{6.0 \cdot \frac{Z}{ZMax} - 3.0 \cdot (1.0 - P) \cdot \left(\frac{Z}{ZMax}\right)^2 - 2.0 \cdot P \cdot \left(\frac{Z}{ZMax}\right)^3}{3.0 + P} \tag{9}$$

where:

| | | |
|---|---|---|
| *AreaFrac* | = | fraction of area of site above given depth (unitless); |
| *VolFrac* | = | fraction of volume of site above given depth (unitless); and |
| *Z* | = | depth of interest (m). |

**Table 2. Examples of Morphometry of Waterbodies**

| Site | ZMean/ZMax | P | Constrained P |
|---|---|---|---|
| *Lakes* | | | |
| Chad, Chad | 0.13 | -2.22 | -1.00 |
| Managua, Nicaragua | 0.26 | -1.42 | -1.00 |
| Michigan, U.S.-Canada | 0.27 | -1.38 | -1.00 |
| Erie, U.S.-Canada | 0.33 | -1.02 | -1.00 |
| Windermere, England | 0.36 | -0.85 | -0.85 |
| Baikal, Russia | 0.43 | -0.42 | -0.42 |
| Como, Italy | 0.45 | -0.30 | -0.30 |
| Superior, U.S.-Canada | 0.47 | -0.18 | -0.18 |
| Tahoe, CA-NV | 0.50 | 0.00 | 0.00 |
| Esrom, Denmark | 0.56 | 0.35 | 0.35 |
| Clear, CA | 0.57 | 0.43 | 0.43 |
| Crater, OR | 0.60 | 0.60 | 0.60 |
| Kinneret, Israel | 0.60 | 0.63 | 0.63 |
| Okeechobee, FL | 0.67 | 1.00 | 1.00 |
| Ontario, U.S.-Canada | 0.69 | 1.14 | 1.00 |
| Balaton, Hungary | 0.75 | 1.50 | 1.00 |
| George, Uganda | 0.80 | 1.80 | 1.00 |
| | | | |
| *Reservoirs* | | | |
| DeGray, AR | 0.25 | -1.49 | -1.00 |
| Grenada, MS | 0.21 | -1.74 | -1.00 |
| Lewis and Clark, SD | 0.31 | -1.13 | -1.00 |
| Texoma, TX | 0.27 | -1.38 | -1.00 |
| Delaware, OH | 0.22 | -1.68 | -1.00 |
| Sidney Lanier, GA | 0.33 | -1.01 | -1.00 |
| Monroe, IN | 0.30 | -1.18 | -1.00 |
| Tenkiller Ferry, OK | 0.36 | -0.86 | -0.86 |
| Mendocino, CA | 0.36 | -0.84 | -0.84 |
| Coralville, IA | 0.37 | -0.80 | -0.80 |
| Waterbury, VT | 0.43 | -0.42 | -0.42 |
| Pend Oreille, ID | 0.50 | -0.03 | -0.03 |
| | | | |
| *Ponds* | | | |
| Czech Rep., fish (very old) | 0.43 | -0.42 | -0.42 |
| Czech Rep., Elbe R. backwaters | 0.50 | -0.03 | -0.03 |
| Dor, Israel, fish, recent | 0.67 | 1.00 | 1.00 |

data from Hutchinson, 1957; Hrbáček, 1966; Leidy and Jenkins, 1977; and Horne and Goldman, 1994

For example, the fraction of the volume that is epilimnion can be computed by setting depth $Z$ to the mixing depth. Furthermore, by setting $Z$ to the depth of the euphotic zone, the fraction of the fraction of the area available for colonization by macrophytes and periphyton can be computed:

$$FracLit = (1 + P) \cdot \frac{ZEuphotic}{ZMax} - P \cdot \left(\frac{ZEuphotic}{ZMax}\right)^2 \quad \textbf{(10)}$$

If the site is a limnocorral (an artificial enclosure) then the available area is increased accordingly:

$$FracLittoral = FracLit \cdot \frac{Area + LimnoWallArea}{Area}$$

otherwise **(11)**

$$FracLittoral = FracLit$$

where:

| | | |
|---|---|---|
| *FracLittoral* | = | fraction of site area that is within the euphotic zone (unitless); |
| *ZEuphotic* | = | depth of the euphotic zone, where primary production exceeds respiration, usually calculated as a function of extinction (m); |
| *Area* | = | site area ($m^2$); and |
| *LimnoWallArea* | = | area of limnocorral walls ($m^2$). |

The depth of the euphotic zone, where radiation is 1% of surface radiation, is computed as (Thomann and Mueller, 1987):

$$ZEuphotic = 4.605/Extinct \quad \textbf{(12)}$$

where:

| | | |
|---|---|---|
| *Extinct* | = | the overall extinction coefficient (1/m), see **(30)**. |

**Figure 13**
Volume as a Function of Depth in Ponds

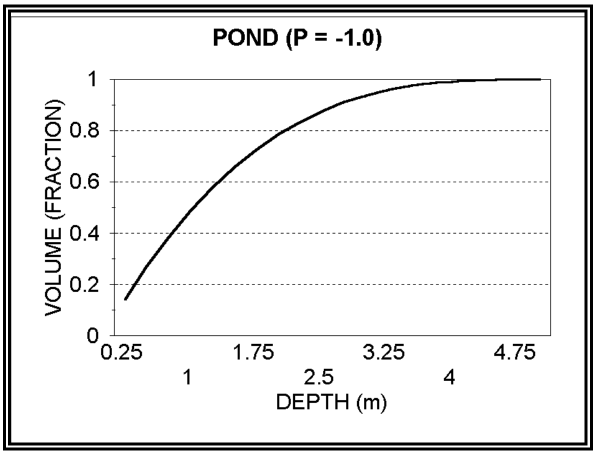


**Figure 14**
Area as a Function of Depth in Ponds

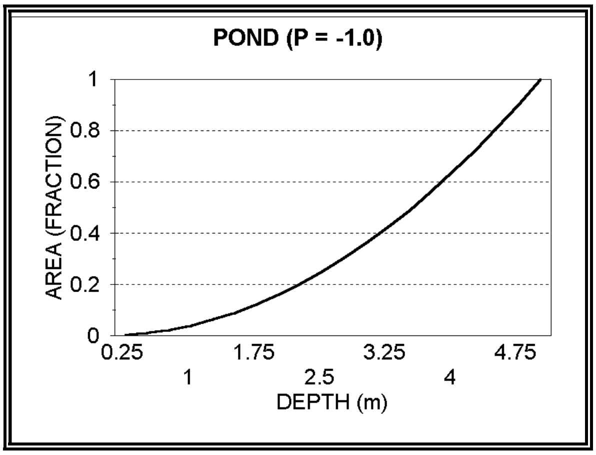

### 3.2 Washout

Transport out of the system, or washout, is an important loss term for nutrients, floating organisms, and dissolved toxicants in reservoirs and streams. Although it is considered separately for several state variables, the process is a general function of discharge:

$$Washout = \frac{Discharge}{Volume} \cdot State \tag{13}$$

where:

| | | |
|---|---|---|
| *Washout* | = | loss due to being carried downstream ($g/m^3 \cdot d$), and |
| *State* | = | concentration of dissolved or floating state variable ($g/m^3$). |

### 3.3 Stratification and Mixing

Thermal stratification is handled in the simplest form consistent with the goals of forecasting the effects of nutrients and toxicants. Lakes and reservoirs are considered in the model to have two vertical zones: epilimnion and hypolimnion (**Figure 15**); the metalimnion zone that separates these is ignored. Instead, the thermocline, or plane of maximum temperature change, is taken as the separator; this is also known as the mixing depth (Hanna, 1990). Dividing the lake into two vertical zones follows the treatment of Imboden (1973), Park et al. (1974), and Straškraba and Gnauck (1983). The onset of stratification is considered to occur when the mean water temperature exceeds 4° and the difference in temperature between the epilimnion and hypolimnion exceeds 3°. Overturn occurs when the temperature of the epilimnion is less than 3°, usually in the fall. Winter stratification is not modeled. For simplicity, the thermocline is assumed to occur at a constant depth.

**Figure 15**
Thermal Stratification in a Lake; Terms Defined in Text

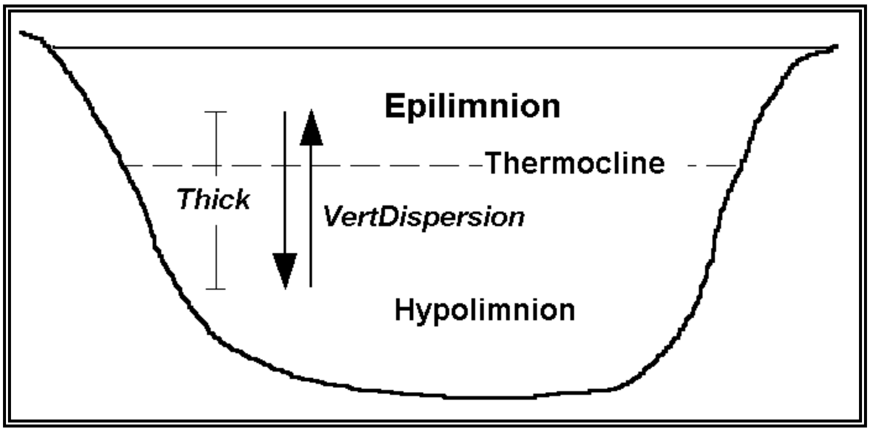


There are numerous empirical models relating thermocline depth to lake characteristics. AQUATOX uses an equation by Hanna (1990), based on the maximum effective length (or fetch). The dataset includes 167 mostly temperate lakes with maximum effective lengths of 172 to 108,000 m and ranging in altitude from 10 to 1897 m. The equation has a coefficient of determination $r^2$ =

0.850, meaning that 85 percent of the sum of squares is explained by the regression. Its curvilinear nature is shown in **Figure 16**, and it is computed as (Hanna, 1990):

$$\log(MaxZMix) = 0.336 \cdot \log(Length) - 0.245 \tag{14}$$

where:

| | | |
|---|---|---|
| *MaxZMix* | = | maximum mixing depth for lake (m); and |
| *Length* | = | maximum effective length for wave setup (m). |

Wind action is implicit in this formulation. Wind has been modeled explicitly by Baca and Arnett (1976, quoted by Bowie et al., 1985), but their approach requires calibration to individual sites, and it is not used here.

Vertical dispersion for bulk mixing is modeled as a function of the time-varying hypolimnetic and epilimnetic temperatures, following the treatment of Thomann and Mueller (1987, p. 203; see also Chapra and Reckhow, 1983, p. 152; **Figure 17**):

$$VertDispersion = Thick \cdot \left( \frac{HypVolume}{ThermoclArea \cdot Deltat} \cdot \frac{|T_{hypo}^{t-1} - T_{hypo}^{t+1}|}{T_{epi}^{t} - T_{hypo}^{t}} \right) \tag{15}$$

where:

| | | |
|---|---|---|
| *VertDispersion* | = | vertical dispersion coefficient ($m^2/d$); |
| *Thick* | = | distance between the centroid of the epilimnion and the centroid of the hypolimnion, effectively the mean depth (m); |
| *HypVolume* | = | volume of the hypolimnion ($m^3$); |
| *ThermoclArea* | = | area of the thermocline ($m^2$); |
| *Deltat* | = | time step (d); |
| $T_{hypo}^{t-1}$, $T_{hypo}^{t+1}$ | = | temperature of hypolimnion one time step before and one time step after present time (°C); and |
| $T_{epi}^{t}$, $T_{hypo}^{t}$ | = | temperature of epilimnion and hypolimnion at present time (°C). |

**Figure 16**
Mixing Depth as a Function of Fetch

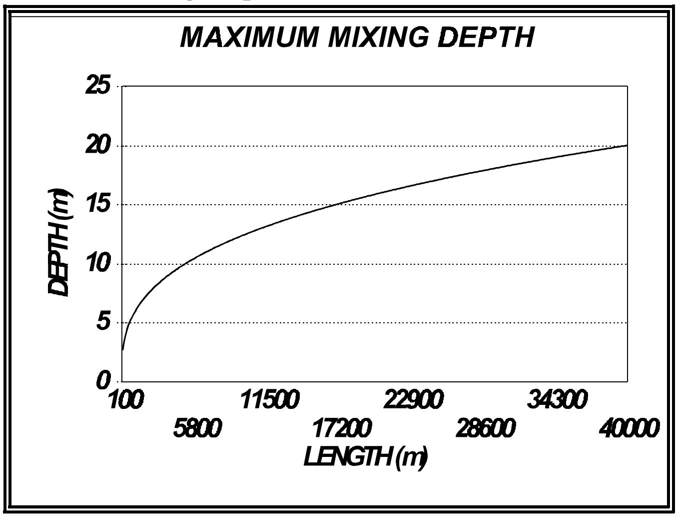


Stratification can break down temporarily as a result of high throughflow. This is represented in the model by making the vertical dispersion coefficient between the layers a function of discharge for sites with retention times of less than or equal to 180 days (**Figure 18**), rather than temperature differences as in equation **15**, based on observations by Straškraba (1973) for a Czech reservoir:

$$VertDispersion = 1.37 \cdot 10^4 \cdot Retention^{-2.269} \tag{16}$$

and:

$$Retention = \frac{Volume}{TotDischarge} \tag{17}$$

where:

| | | |
|---|---|---|
| *Retention* | = | retention time (d); |
| *Volume* | = | volume of site ($m^3$); and |
| *TotDischarge* | = | total discharge ($m^3$/d). |

**Figure 17**
Vertical Dispersion as a Function of Temperature Differences

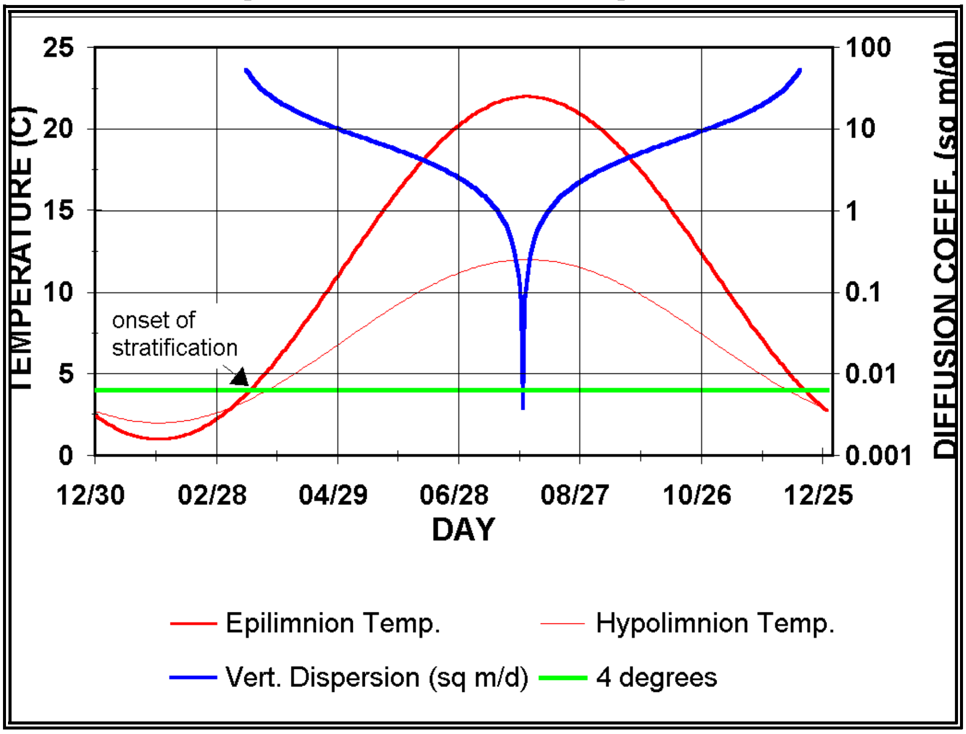


**Figure 18**
Vertical Dispersion as a Function of Retention Time

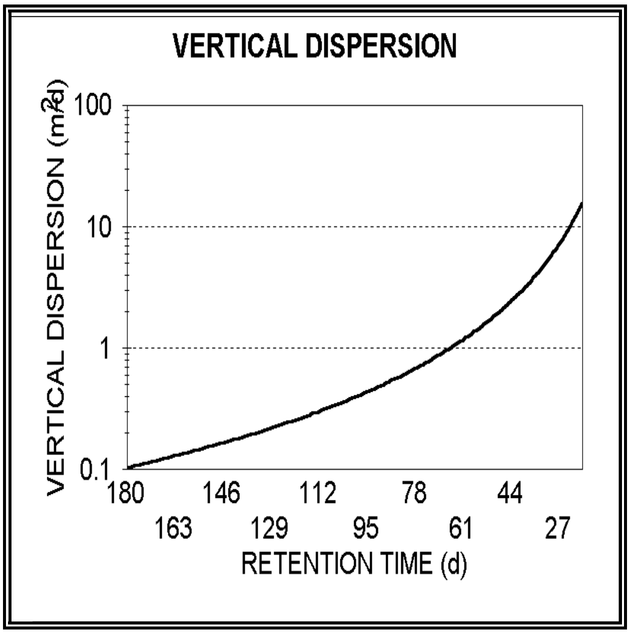


The bulk vertical mixing coefficient is computed using site characteristics and the time-varying vertical dispersion (Thomann and Mueller, 1987):

$$BulkMixCoeff = \frac{VertDispersion \cdot ThermoclArea}{Thick} \tag{18}$$

where:

*BulkMixCoeff* = bulk vertical mixing coefficient ($m^3/d$),
*ThermoclArea* = area of thermocline ($m^2$).

Turbulent diffusion between epilimnion and hypolimnion is computed separately for each segment for each time step while there is stratification:

$$TurbDiff_{epi} = \frac{BulkMixCoeff}{Volume_{epi}} \cdot (Conc_{compartment,\ hypo} - Conc_{compartment,\ epi}) \tag{19}$$

$$TurbDiff_{hypo} = \frac{BulkMixCoeff}{Volume_{hypo}} \cdot (Conc_{compartment,\ epi} - Conc_{compartment,\ hypo}) \tag{20}$$

where:

*TurbDiff* = turbulent diffusion for a given zone ($g/m^3 \cdot d$);
*Volume* = volume of given segment ($m^3$); and
*Conc* = concentration of given compartment in given zone ($g/m^3$).

The effects of stratification, mixing due to high throughflow, and overturn are well illustrated by the pattern of dissolved oxygen levels in the hypolimnion of Lake Nockamixon, a eutrophic reservoir in Pennsylvania (**Figure 19**).

**Figure 19**
Stratification and Mixing in Lake Nockamixon,
Pennsylvania as Shown by Hypolimnetic Dissolved Oxygen

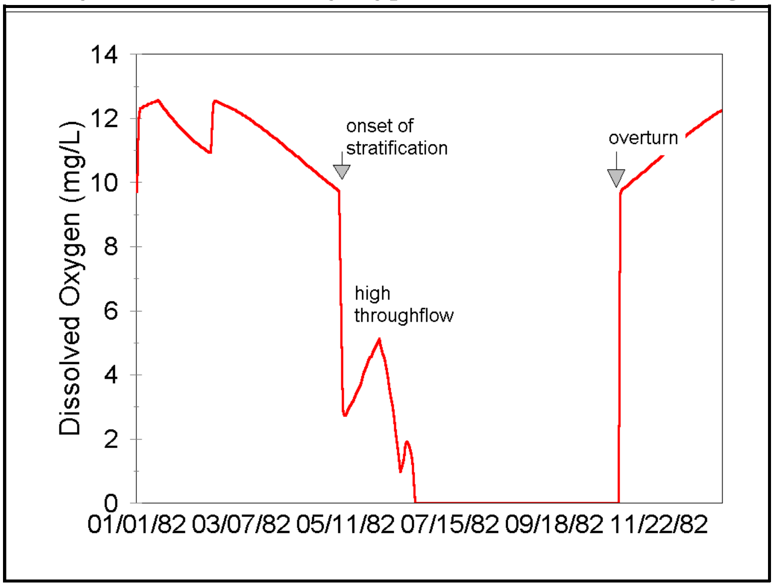


## 3.4 Temperature

Default water temperature loadings for the epilimnion and hypolimnion are represented through a simple sine approximation for seasonal variations (Ward, 1963) based on user-supplied observed means and ranges (**Figure 20**):

$$Temperature = TempMean + (-1.0 \cdot \frac{TempRange}{2} \cdot (\sin(0.0174533 \cdot (0.987 \cdot (Day + PhaseShift) - 30))))] \quad \textbf{(21)}$$

where:

| | | |
|---|---|---|
| *Temperature* | = | average daily water temperature (°C); |
| *TempMean* | = | mean annual temperature (°C); |
| *TempRange* | = | annual temperature range (°C), |
| *Day* | = | Julian date (d); and |
| *PhaseShift* | = | time lag in heating (= 90 d). |

Observed temperature loadings should be entered if responses to short-term variations are of interest. This is especially important if the timing of the onset of stratification is critical, because stratification is a function of the difference in hypolimnetic and epilimnetic temperatures (see **Figure 18**).

### 3.5 Light

The default incident light function is a variation on the temperature equation, but without the lag term:

$$Solar = LightMean + \frac{LightRange}{2} \cdot \sin(0.0174533 \cdot Day - 1.76) \tag{22}$$

where:

| | | |
|---|---|---|
| *Solar* | = | average daily incident light intensity (ly/d); |
| *LightMean* | = | mean annual light intensity (ly/d); |
| *LightRange* | = | annual range in light intensity (ly/d); and |
| *Day* | = | Julian date (d). |

The derived values are given as average light intensity in Langleys per day (Ly/d = 10 kcal/$m^2 \cdot d$). An observed time-series of light also can be supplied by the user; this is especially important if the effects of daily climatic conditions are of interest. If the average water temperature drops below 3°C, the model assumes the presence of ice cover and decreases light to 33% of incident radiation. This reduction, due to the reflectivity and transmissivity of ice and snow, is an average of widely varying values summarized by Wetzel (1975; also see LeCren and Lowe-McConnell, 1980). The model does not automatically adjust for shading by riparian vegetation, so a times-series should probably be supplied if modeling a narrow stream.

Photoperiod is approximated using the Julian date (**Figure 21**):

$$Photoperiod = \frac{12 + A \cdot \cos(380 \cdot \frac{Day}{365} + 248)}{24} \tag{23}$$

where:

| | | |
|---|---|---|
| *Photoperiod* | = | fraction of the day with daylight (unitless); |
| *A* | = | hours of daylight minus 12 (hr); and |
| *Day* | = | Julian date (d). |

*A* is the difference between the number of hours of daylight at the summer solstice at a given latitude and the vernal equinox, and is given by a linear regression developed by Groden (1977):

$$A = 0.1414 \cdot Latitude - Sign \cdot 2.413 \tag{24}$$

where:

| | | |
|---|---|---|
| *Latitude* | = | latitude (°, decimal), negative in southern hemisphere; and |
| *Sign* | = | 1.0 in northern hemisphere, -1.0 in southern hemisphere. |

**Figure 20**
Annual Temperature

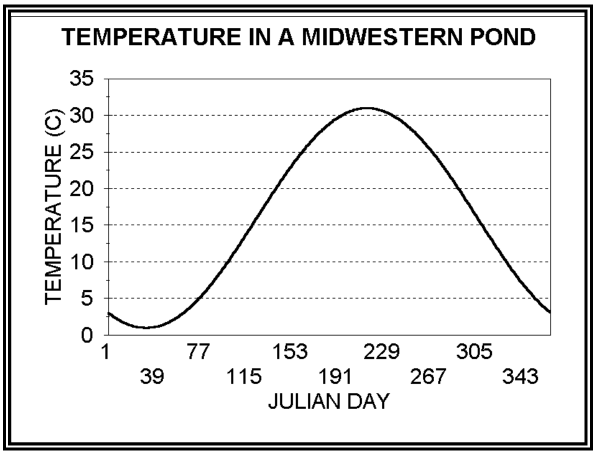


**Figure 21**
Photoperiod as a Function of Date

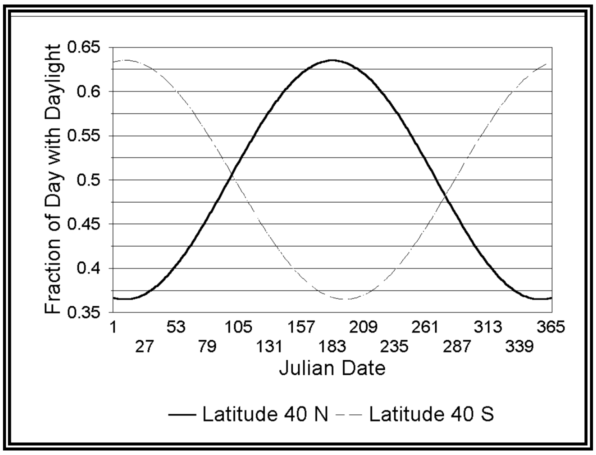


### 3.6 Wind

Wind is an important driving variable because it determines the stability of blue-green algal blooms, and reaeration or oxygen exchange, and it controls volatilization of some organic chemicals. If site data are not available, default variable wind speeds are represented through a Fourier series of sine and cosine terms; the mean and first ten harmonics seem to capture the variation adequately (**Figure 22**). This default loading is based on an unpublished 140-day record (May 20 to October 12) from Columbia, Missouri; therefore, it has a 140-day repeat, representative of the Midwest during the growing season. This approach is quite useful because the mean can be specified by the user and the variability will be imposed by the function. If ice cover is predicted, wind is set to 0.

**Figure 22**
Default Wind Loadings for Missouri Pond